EFDA–JET–PR(09)50

F.P. Orsitto, A. Boboc, P. Gaudio, M. Gelfusa, E. Giovannozzi, C. Mazzotta,
A. Murari and JET EFDA contributors

Analysis of Faraday Rotation in JET Polarimetric Measurements

Analysis of Faraday Rotation in JET Polarimetric Measurements

F.P. Orsitto[1], A. Boboc[2], P. Gaudio[3], M. Gelfusa[3], E. Giovannozzi[1], C. Mazzotta[1], A. Murari[4] and JET EFDA contributors*

JET-EFDA, Culham Science Centre, OX14 3DB, Abingdon, UK

[1]Associazione EURATOM-ENEA C R Frascati 00044 Frascati, Italy
[2]EURATOM-CCFE Fusion Association, Culham Science Centre, OX14 3DB, Abingdon, OXON, UK
[3]Associazione EURATOM-ENEA, Università Roma II Tor Vergata, Italy
[4]Associazione EURATOM-ENEA sulla Fusione, Consorzio RFX Padova, Italy
** See annex of F. Romanelli et al, "Overview of JET Results",*
(Proc. 22 [nd] IAEA Fusion Energy Conference, Geneva, Switzerland (2008)).

Preprint of Paper to be submitted for publication in
Plasma Physics and Controlled Fusion

ABSTRACT

The paper deals with JET polarimeter measurements and in particular it presents a study of the *Faraday rotation* angle, which is used as constraint in equilibrium codes. This angle can be calculated by means of the rigorous numerical solution of Stokes equations. A detailed comparison is done of calculations with the time traces of measurements, inside a limited dataset representative of JET discharges: in general it is found that the Faraday rotation angle and Cotton-Mouton phase shift measurements can be represented by the numerical solution to Stokes equations. To get this agreement in particular for Faraday rotation, a shift of the magnetic surfaces must be included. This results in improvement of the position of the magnetic surfaces as calculated by EFIT equilibrium code. The approximated *linear* models normally used can be applied only at low density and current. The Cotton-Mouton is calculated at high plasma density including the contribution by Faraday rotation angle. For high plasma current the non-linear terms in the propagation equations can be important. These conclusions have some impact on the mathematical form of the polarimetric constraints (Faraday and Cotton-Mouton) in equilibrium codes.

1. INTRODUCTION

The measurements of polarimetry in tokamak plasmas can give important information on plasma current and density [1]. In a plasma, in presence of a magnetic field, the polarization plane of a laser beam propagating along the magnetic field rotates (Faraday effect). Whereas, if the laser beam is propagating perpendicular to the magnetic field there is a change in the ellipticity of the polarization (Cotton-Mouton effect). In a beam propagating vertically along a line in a poloidal plane of a tokamak , both effects are presents: the polarization becomes elliptical and the plane of the polarization rotates.

As a first approximation, it is possible to consider the two effects as being independent: the Faraday effect depending only on the magnetic field parallel to the beam direction times the plasma density, while the Cotton-Mouton depending on the plasma density and the perpendicular (to the line of sight) magnetic field squared. Since the structure of the propagation equations of polarization inside the plasma in the magnetic field of a tokamak couples the Faraday and Cotton-Mouton, the two effects must be taken into account at the same time, in a rigorous approach to calculate the change of polarization of a laser beam.

In a previous paper [2], the analysis of Cotton-Mouton measurements was carried out and the consistency of measurements with the Stokes equation models was assessed. It was shown that the Cotton-Mouton phase shift angle can be calculated by means of the rigorous solution of Stokes equations, which define the spatial evolution of the polarisation of the laser beam inside the plasma. The coupling between Faraday and Cotton-Mouton was demonstrated important for large Faraday effects. In fact, to analyze the coupling between Faraday and Cotton-Mouton a new approximate analytic solution (Type II)[2] was introduced. Using the topology of tokamak magnetic fields, an ordering was found between the components of the vector $\vec{\Omega}$ appearing in the Stokes equations (see sec 2), leading to a simplified analytic solution, which exhibits i) a sensible dependence of the Cotton-Mouton phase shift upon the

Faraday rotation angle, while ii) the Faraday rotation is not depending on Cotton-Mouton (see comments to [II.12]).

In the present paper the analysis of Faraday rotation measurements is carried out, following the same method developed in [2], using the Stokes equations and their numerical and approximate solutions. The coupling between Faraday and Cotton-Mouton is analyzed further, from the general point of view, using a new set of non-linear equations derived from the Stokes ones.

The main questions, which are addressed in the present paper, are : i) which is the most suitable model for the Faraday rotation measurements on JET and the possible improvement to the equilibrium calculation which can be obtained through the comparison between the measurements and the numerical solution of Stokes equations (see sec.3 and 4) ; ii) how the coupling acts on Faraday and Cotton-Mouton, i.e. whether the dependence found using Type II solution is general (see sec 5 and 6). Both points are relevant to the modelling of Faraday rotation and Cotton-Mouton effects to be used as constraints in equilibrium codes.

To answer to the previous questions, the data from JET polarimetric system are used : few discharges are studied representative of regimes where the polarimetric effects are reasonably strong (see Table I and III).

This paper presents a comprehensive study of the following aspects: i) a detailed analysis of Faraday measurements at JET and comparison with available models. It turns out that the Faraday rotation measurements on JET can be reproduced in any condition **only** by the numerical solution of Stokes equations and by a suitable shift of the magnetic surfaces. A specific study shows that the comparison between model calculations and measurements lead to a more refined identification of the positions of the magnetic surfaces as predicted by EFIT equilibrium code[3] ; ii) a rigorous approach to the interaction between Faraday and Cotton-Mouton, (studied in recent papers, see ref [2] for details): it is demonstrated that at **high density and current**, the Cotton-Mouton **must** be calculated including the dependence by Faraday rotation.

Since the solutions to the Stokes equations were discussed in [2], the names and classification of the solutions are retained in the present paper, and only a short introduction to Stokes equations and solutions will be presented, the details are given in ref[2].

The paper is organized as follows: in sec.2, a short summary of the measurements of JET polarimetry system is given, together with the Stokes equations and their approximate solutions; in sec. 3, the analysis of Faraday rotation measurements is presented comparing measurements and solutions of the Stokes equations for few typical JET discharges, where to reconcile the measurements with the calculations a shift of the magnetic surfaces is needed; in sec.4, a statistical analysis on large databases of the determination of the shift is presented; in sec.5, the mutual interaction between Faraday rotation and Cotton-Mouton for a high density shot is presented; in sec.6, a theoretical analysis of the coupling between Faraday and Cotton-Mouton effects and its application to study shots with high density and high

plasma current is presented. The coupling between Faraday and Cotton-Mouton is analyzed using a new set of equations (derived from the Stokes equations) which are useful to understand how the coupling acts; in sec.VII, comments are presented on the mathematical models of Faraday and Cotton-Mouton to be used as constraints in equilibrium codes; in sec.VIII, the conclusions are presented.

Hereafter a plasma discharge is named also using 'shot'; and 'numerical solution' is always referred to the numerical solution of the Stokes equations (see equations [2.2.]) , using as input to the equations, the density profile measured by Thomson scattering and the magnetic fields calculated by the EFIT equilibrium code[3], (see sec.II); the terms 'Faraday' ('Cotton-Mouton') will be used often, meaning 'Faraday rotation angle' ('Cotton-Mouton phase shift angle') measurements. In the paper the symbols φT and ψT are used for the Cotton-Mouton phase shift and Faraday rotation angle respectively obtained by numerical solutions of Stokes equations.

2. STOKES EQUATIONS AND THEIR APPROXIMATE SOLUTIONS.

The considered geometry includes the propagation of a laser beam along a vertical chord (taken as z-axis) in a poloidal plane of a Tokamak. The toroidal magnetic field ($\vec{B}_t$) is perpendicular to this plane and the angle of the electric field vector of the input wave with $\vec{B}_t$ is 45^0. The polarisation of a beam can be described using the Stokes vector $\vec{s}$, whose components are expressed in terms of the ellipticity angle (χ) and Faraday angle (ψ), or in terms of the ratio of the components of the laser beam electric field (α) and their phase shift angle (φ).

The equations defining the Stokes vector $\vec{s} = (s_1, s_2, s_3)$ are :

$$
\begin{aligned}
s_1 &= \cos(2\chi)\cos(2\psi) = \cos(2\alpha) \\
s_2 &= \cos(2\chi)\sin(2\psi) = \sin(2\alpha)\cos(\varphi) \\
s_3 &= \sin(2\chi) = \sin(2\alpha)\sin(\varphi) \\
s_1^{\,2} + s_2^{\,2} + s_3^{\,2} &= 1
\end{aligned}
\qquad [2.1]
$$

It is worth remembering that the JET polarimeter system measures primarily i) two components of the electric field (Ex and Ey, in a plane orthogonal to the propagation direction) of the laser beam emerging from the plasma as well as ii) the phase shift (φ) between these components. So the primary measurements are

$$\alpha = \frac{Ey}{Ex} \quad and \quad \varphi$$

In principle the JET polarimetric system gives the possibility of determining directly the values of the components of the Stokes vector, using the measurements of α and φ and the definitions [2.1].

The Faraday rotation is obtained using the relation :

$$\tan 2\psi = \tan 2\alpha \cos\varphi$$

and the ellipticity , defined as $\varepsilon = \tan\chi$, is obtained by the formula :

$$\tan 2\chi = \frac{s_3}{\sqrt{1 - s_3^{\,2}}}$$

The spatial evolution along the z-axis of the polarization of a beam is given by the Stokes equation :

$$\frac{d\vec{s}}{dZ} = \vec{\Omega} \times \vec{s} \qquad [2.2]$$

where

$$\vec{\Omega} = ka\left(\Omega_1, \Omega_2, \Omega_3\right), \text{ and } \Omega_1 = C_1 n (B_t^2 - B_x^2); \quad \Omega_2 = 2C_1 n B_x B_t; \; \Omega_3 = C_3 n B_z \qquad [2.3]$$

B_t is the toroidal magnetic field (Tesla), B_z the component of the poloidal magnetic field along the propagation axis, B_x the component of poloidal magnetic field orthogonal to the propagation axis (the ratio $B_x/B_t \leq 10^{-1}$, so neglecting B_x implies an error ≤1% in the evaluation of Ω_1), n is the electron density (m^{-3}), $C_1 = 1.8\times10^{-22}$ and $C_3 = 2\times10^{-20}$, calculated for the laser wavelength of λ = 195 μm, and Z = z/ka is the normalized coordinate along a vertical chord, where k is the elongation and a the minor radius. The relations between the Faraday rotation ψ and the Cotton-Mouton phase shift φ angles and the corresponding components of Stokes vector follow from [2.1]:

$$\frac{s_2}{s_1} = \tan 2\psi \qquad [2.4]$$

$$\frac{s_3}{s_2} = \tan\varphi \qquad [2.5]$$

Equations [II.2] are solved , with the initial condition :

$$\vec{s}_0 = (0,1,0) \qquad [2.6]$$

corresponding to 45^0 angle between the electric field vector of the input wave and $\vec{B}_t$.

In the present work data related to the channel #3 (corresponding to the vertical line with coordinate R= 3.04 m, r/a~0.04) and channel #4 (a vertical line with coordinate R=3.74m, approximately tangent to the last closed magnetic surface) are presented: the data exhibit a reasonably good signal to noise ratio and the geometry to be analyzed is relatively simple.

The values of the vector $\vec{\Omega} = ka\left(\Omega_1, \Omega_2, \Omega_3\right)$ are obtained [2] using the values of $\vec{B}$ as calculated by the EFIT equilibrium reconstruction and the LIDAR Thomson Scattering measurements of plasma density (n) projected along the line of sight of the vertical channels on the basis of the reconstructed equilibrium.

The type I solution [2], to the Stokes equations [2.2], is found if the quantities $W_3 = \int \Omega_3 dz = C_3 \int n_e B_z dz$ and $W_1 = \int \Omega_1 dz = C_1 \int B_t^2 n_e dz$ satisfy to the conditions $W_i^2 << 1$ (in the definition of W_1, the component B_x has been neglected, see [2.3]), and $W_2 << W_1$.

The type I solution is obtained as the first term of a series expansion to the solution of the system of ordinary differential equations [2.2], together with the initial condition [2.6]. In this approximation the relations between the Stokes vector, the Faraday rotation ψ and Cotton-Mouton phase shift angle ϕ are given by:

$$s_1 = - W_3 = C_3 \int n_e B_z dz = 1 / \tan 2\psi \qquad [2.7]$$

$$s_2 = 1 - (W_1^2 + W_3^2)/2 \approx 1 \qquad [2.8]$$

$$s_3 = W_1 = C_1 \int B_t^2 n_e dz = \tan\varphi \qquad [2.9]$$

Relations [2.7] and [2.9] are the key equations used for evaluating the polarimetric measurements linking the Faraday rotation to the component of the poloidal magnetic field along the direction of propagation of the laser beam (and then to the plasma current profile), and the Cotton-Mouton phase shift angle to the line–integral of the electron density. The expressions in [2.7] and [2.9] are valid only for $W_i^2 << 1$: for large Faraday and Cotton-Mouton angles (see also in the following the discussion on Type II approximation) other methods must be used to find solutions to the Stokes equations. The term of 'linear approximation' will be used in this paper with reference to formulas [2.7-9].

The physical meaning of the type I approximation can be appreciated, if we consider the situation where the transverse components of the magnetic field are not present , (i.e. $B_t = B_x = 0$ in [2.3], and $\Omega_1 = \Omega_2 = 0$), and there is a magnetic field B_z in the direction of beam propagation. This is the case of a 'pure' Faraday rotation. Solving the Stokes equations [2.2] with the initial conditions [2.6] leads to the solutions :

$$s_1 = \cos 2\psi = \cos(2\psi_0 + W_3)$$
$$s_2 = \sin 2\psi = \sin(2\psi_0 + W_3)$$
$$s_3 = \sin 2\chi_0 = 0$$

the Faraday rotation is then obtained from the previous equations :

$$2\psi = 2\psi_0 + W_3$$

It can be verified that the previous formula leads to the 2.7](Type I) at the same level of the approximation (i.e. $W_3 << 1$, in practice $W_3 << \pi/6 = 0.5$) . The 'pure ' Faraday rotation is represented by $W_3/2$.

The 'pure Cotton-Mouton' can be derived from the solutions of Stokes equations considering the case of $B_z = Bx = 0$, i.e. $\Omega_3 = 0 = \Omega_2$:

$$s_1 = s_{1_0} = 0$$
$$s_2 = \sin 2\alpha_0 \cos\varphi = \sin 2\alpha_0 \ \cos(\varphi_0 + W_1) = \cos(\varphi_0 + W_1)$$
$$s_3 = \sin 2\alpha_0 \ \sin\varphi = \sin 2\alpha_0 \ \sin(\varphi_0 + W_1) \ = \sin(\varphi_0 + W_1)$$

The 'pure Cotton-Mouton ' is then represented by W_1, in fact from the previous equations we obtain:

$$\varphi = \varphi_0 + W_1$$

In the ideal conditions $\varphi_0 = 0$, so $\varphi = W_1$.

The physical meaning of W_1 and W_3 is related with 'pure' Cotton-Mouton and Faraday rotation respectively, in a context where the two effects can be considered separately and possibly independent.

More general approximate solutions[2] to the equations [2.2] can be found, observing that the following inequalities between the components of the vector $\vec{\Omega}$ hold for Tokamak plasmas:

$$\left|\Omega_3\right| \ \geqslant \ \Omega_1 > \left|\Omega_2\right| \qquad [2.10].$$

As consequence of the condition [2.10], the terms with component Ω_2 can be neglected in the Stokes equations [2.2] and terms in $\Omega_1 s_3$ neglected with respect to $\Omega_3 s_1$, in this approximations the Stokes equations can be integrated analytically, and the expressions (Type II solutions) for the Faraday angle and Cotton-Mouton phase shift can be obtained [2]:

$$\frac{s_2}{s_1}(z) = \tan 2\psi = -\frac{1}{\tan(W_3)} \quad ; \frac{s_3}{s_2}(z) = \tan\phi = \frac{\int_{-z}^{+z} dy \Omega_1(y)\cos(W_3(y))}{\cos(W_3(z))} \qquad [2.12]$$

A clear trend present in the formulas [2.12] is that the Cotton-Mouton phase shift increases with W_3, (for values correspoding to JET data), (see sec 3 and fig.6). In practice for Faraday rotation angles $\psi \leq 12^o$, $1 \geq \cos(W3) \geq 0.9$ and $\tan\varphi \approx W1$, within an approximation of 10%, whereas for Faraday angles higher than 12^o the Cotton-Mouton increases due to the enhancement linked with Faraday rotation($W_3 \geq \pi/15 = 0.2$).

In the following discussion concerning the comparison between measurements and model calculations, the Guenther ModelA [4] will be cited as well : a discussion of the details of this model is given in [2,5].

3. FARADAY ROTATION MEASUREMENTS AND COMPARISON WITH MODELS.

Examples of the calculations of the Faraday effect can be produced by starting from data of shots representative of JET typical operational space. Table I gives a choice of three shots with parameters from low density/low current , to high density/ high current. Table II summarizes the values of the experimental errors in the measurements used in the Stokes equations.

Figure1 shows the numerical solution of Stokes equations($1/\tan 2\psi$ T), together with the Faraday measurements($1/\tan 2\psi$ ex) for the shot# 60980: the numerical solution agrees with measurements within the errorbar, which for Faraday rotation angle is $\Delta\psi$=0.004rad(0.22^o).

Figure 2 shows the comparison between Faraday measurements and the approximate solutions (Type I [2.7-9] , Type II [II.11] and Guenther ModelA (W3G)). All the models are in agreement with the measurements. In particular Type I reproduces the data and this is expected due to the low value of the Faraday angle and corresponding W_3. This is the case of 'pure' Faraday effect.

Moving to the high density shot #67777 , fig.3 shows the calculations for the Faraday rotation corresponding to channel#3. The values of the spatial profile of B_z(z, Rchannel) (Rchannel is the radial coordinate of the vertical chord, z the coordinate along the chord) is critical for the determination of the Faraday rotation: we find that the equilibrium in agreement with the measurements of polarimetry corresponds to **a shift of 0.035m of the magnetic surfaces** in the direction of high field side. In this conditions we find that all the models (also the 'linear' model W_3) are in agreement with the measurements.

The equilibrium used in the previous calculations is evaluated including only magnetic measurements, the question araises to whether an equilibrium evaluated using constraints from polarimetry could improve the prediction of Faraday rotation as calculated by the Stokes equations, without needing a shift. To answer to this question an equilibrium was generated by EFIT where the minimization was obtained including the constraint of Faraday rotation, but a shift of 0.035m was still needed to reconcile the measurement with the calculations.

To study further this problem the comparison between data and calculations were carried out for a shot#76846(BT/Ip=1.7T/1.4MA, ne=5.5 $10^{19}m^{-3}$,Te=4.5keV), with two types of equilibria: i) EFIT equilibrium obtained using only magnetic measurements (IEFIT); ii) EFIT equilibrium obtained using constraints which include MSE(Motional Stark Effect) measurements and pressure measurements (performed by the High resolution Thomson scattering system) (EFTM) . Fig.3a shows the comparison between calculations and data using IEFIT, and fig.3c shows the results of comparison when the shift DR=0.045m is introduced, using IEFIT equilibrium. Fig.3b shows the comparison (between Faraday data and calculations) using the constrained equilibrium EFTM: it can be noted that using EFTM an

improvement is obtained, but this is not enough to obtain an agreement between measurements and calculations. The agreement is found only introducing a rigid shift of the magnetic surfaces of DR=0.02m when EFTM is used(see fig.3d). The figures 3 are corresponding to measurements of channel #3.

Thus using a more refined equilibrium like EFTM, which includes internal measurements (MSE and pressure profiles) as constraints, leads to a reduction of the shift of the magnetic surfaces (DR=0.02m instead of DR=0.04m) needed to reconcile polarimetry model and measurements.

In more detail, the previous figures show that : i) the comparison between the calculations and measurements of Faraday rotation can give important informations about the accuracy of equilibrium calculations; ii) the comparison can be used to improve the calculations of the position of the equilibrium surfaces: in practice the calculation of the Faraday rotation angle using Stokes model is useful to evaluate how to shift the flux surfaces to improve the evaluation of the equilibrium.

The same procedure must be applied to the calculations related to the channel#4 which is the outermost vertical channel with coordinate R=3.74m, leading to a shift DR=0.04m (for the shot #67777). This is not expected because the equilibrium is supposed to be accurate at plasma edge, where the magnetic sensors are placed. Data related to channel#4 are shown in the fig.4 from the top : the first plot shows a comparison between the numerical calculations and measurements, the second plot the measurements compared with Type II model, and the third the comparison between the measurements and the Type I and Guenther Model A.

In practice *the numerical model and the Type II are in agreement with data,* while Type I and Guenther Model A underestimate the Faraday measurements. The Faraday measurements give a rotation quite large (as it can be expected) on channel#4 of the order of 23^{o} , and a value of W3≈1: we find in fact that Type I (which is a measurement of 'pure Faraday ' rotation) is not a good approximation. This experimental finding confirms the conclusions drawn from the TypeII model in sec.II.

4. STATISTICAL ANALYSIS OF THE 'SHIFT' OF THE MAGNETIC SURFACES.

A statistical analysis on a large database of shots including measurements of years 2003-2007 confirms the procedure outlined for the shot# 67777. In particular a database was built (see table III) to study the dependence upon the main plasma parameters (plasma density, current and toroidal magnetic field), of the shift of the magnetic surfaces needed to reconcile the Faraday measurements with the calculations . The study was limited to data of channel#3. The equilibrium used was EFIT with magnetic measurements only.

For each shot (see Table III), the shift was determined by the minimization of the χ^2, build using the Faraday measurements and the corresponding values obtained by solving the Stokes equations.

The result of the analysis is shown in figures 5a-5c: fig.5a is a plot of the shift versus the maximum line averaged electron density measured by LIDAR Thomson Scattering ; fig.5b is a plot of the shift versus the plasma current ; and fig.5c shows the shift versus the ratio BT/IP (toroidal magnetic field /

plasma current). The calculated shift, ranging in the interval DR=0.01-0.05m, **does not exhibit** any strong dependence upon plasma parameters.

An extensive statistical analysis (based on validated shots belonging to campaigns of years 2007-2009) on the shift was carried out for the measurements of channel #4 (the outermost vertical channel with coordinate R=3.74m). In the calculations of the Stokes equations the density profile used were measured by the HRTS(High Resolution Thomson Scattering) , which has a spatial resolution at edge of the order of 0.015m. The average shift calculated was of the order of DR=0.02m.

The shift needed is likely due to the accuracy of the EFIT equilibrium calculations, in terms of space resolution. This is limited by the dimension of the elements of the grid used by EFIT [6]: the element has a dimension dZ X dR = 0.126 X 0.075 m^2,(dZ (dR) is the dimension in the vertical(radial) direction),. *The shift found then in the study presented in this paper is consistent with the radial space resolution of the EFIT calculations.*

From these data it is important to realize that the comparison between calculation and measurement of Faraday rotation lead to a strong improvement of the evaluation of the position of the magnetic surfaces.

To confirm that the EFIT calculations can be affected by a certain systematic uncertainty, a comparison of the average radial location of the lower outer strike point as predicted by EFIT and XLOC was done, using a large database of 460 shots chosen in 2003-2007 years.

The code XLOC[7] is a simplified equilibrium code which is used for the determination of the X-point location and strike points of the open field lines derived from the X-point on the divertor tiles.

The result obtained after this comparison is that EFIT predicts a position of the lower outer strike point systematically in excess of 0.06 m with respect to XLOC calculations , confirming the shift in the same direction detected using the polarimetry analysis.

5. COTTON-MOUTON VERSUS FARADAY ROTATION IN A HIGH DENSITY SHOT.

Since for shot#67777 the Faraday rotation angle is significant, it is instructive to see whether for calculating the Cotton-Mouton phase shift the Type I approximation would be enough. The level of disagreement between the Type I approximation and the measurement can be considered as an 'interference' of the Faraday rotation on the Cotton-Mouton effect (in the sense already discussed in sec.II, in relation to the Type II approximation). A comparison between the Cotton-Mouton phase shift measured (for shot#67777, ch#3, blue line), the numerical solution (green star) and the calculation of W_1 (red circles) is given in fig.6: the Type I approximation (where $W_{1max} \approx 0.35$) is not enough to evaluate the Cotton-Mouton measurements , since it underestimates the value of tanφ by 30%. In this case there is an interference of the Faraday effect which results in a contribution of 30% to the Cotton-Mouton effect: the measurement of the Cotton-Mouton effect cannot be reconciled in the case of high density to a 'pure' effect.

The effect of Faraday rotation on Cotton-Mouton can be observed also in fig.7: the ratio tanφT /W_1 (for the shot #67777, channel#4) is plotted versus W_3 to detect the departure of Cotton-Mouton phase shift angle from linearity, in relation with the level of Faraday rotation, which is measured by W_3. It turns out that the Cotton-Mouton phase shift exceeds substantially the 'linear' evaluations already for values W_3>0.4. This finding is in agreement with the general trend predicted by the Type II approximation.

6. THEORETICAL ANALYSIS OF THE COUPLING BETWEEN FARADAY AND COTTON-MOUTON EFFECTS AND APPLICATION TO STUDY SHOTS AT HIGH DENSITY AND HIGH PLASMA CURRENT.

In the previous section a demonstration of the coupling between Faraday and Cotton-Mouton was shown comparing the Type I approximation (which represents 'pure' effects) with measurements.
We have found that for a high density shot the Faraday as well as Cotton-Mouton measurements cannot be obtained using the 'linear formulas' (Type I). In this section a short theoretical discussion will be presented about the coupling.

In this section a short theoretical discussion will be presented about the coupling.

Moving to a more general analysis , we start from the Stokes equations [II.2] to derive equations where the coupling terms between Faraday and Cotton-Mouton can be clearly identified.
Defining

$$F = \frac{s_1}{s_2} = \frac{1}{\tan 2\psi} \quad and \quad C = \frac{s_3}{s_2} = \tan\varphi$$

from the Stokes equations [II.2] the following system can be derived :

$$\frac{dF}{dZ} = -\Omega_3 - \Omega_3 F^2 + \Omega_1 F C + \Omega_2 C \qquad [3.1]$$

$$\frac{dC}{dZ} = \Omega_1 + \Omega_1 C^2 - \Omega_3 F C - \Omega_2 F \qquad [3.2]$$

The system [III.1-2] can be considered as a generalized Volterra-like problem, with non-constant coefficients. The propagation of polarization in a plasma can be described using a first order non-linear differential system in two variables: plasma polarimetry is intrinsically described by a **bidimensional dynamical system**, so chaotic behaviour cannot be realized.

The magnitude of the terms at the right hand side of [3.1-2] can be estimated solving directly the Stokes equations. The fig.8a and b show how the non-linear terms play in the determination of Cotton-Mouton effect: the values of dC/dZ and Ω_1 are plotted together versus the normalized coordinate along the beam path for the channel #3 (fig.8a) and channel#4(fig.8b) at the time t=18s , for the high density

shot #67777: it appears that the non-linear terms become important for Z>0. The fig.9a and 9b show a similar plot for the Faraday rotation angle, the values of dF/dZ and Ω_3 are plotted together for shot#67777 : it appears that the non-linear terms are negligible for the channel#3(fig.9a), while the non-linear terms are important for channel#4(fig.9b).

It has been verified that the most important non-linear term for Faraday is the term $\Omega_3 F^2$, while for Cotton-Mouton is the term Ω_3 FC, in eq.[3.1-2].

Figure10a and 10b and 11a and 11b simulate a **high current** , high density shot (#75238): the same trend (as for shot#67777, channel#3 and 4) is detected. In particular for the Cotton-Mouton (fig.10) the non-linear terms are important for Z>0: this is evident for channel#3(fig.10a), but it is remarcable for channel#4 (fig.10b). For the Faraday rotation angle, the fig.11a shows that for Z>0 a small difference appears, in channel#3, between the exact value of Faraday rotation derivative and the value of Ω_3, the fig.11b shows that for channel#4 the non-linear F^2 term is dominant.

The importance of non-linear terms for Faraday rotation is confirmed by a comparison between the Faraday rotation measurements and the calculations as shown in fig.12, where the experimental data(blue line) are shown together with the numerical calculation (red continuous line) and the linear formula (green crosses): the value of W_3 slightly underestimate the Faraday measurement for the high current shot, while the numerical solution is in agreement with the measured Faraday rotation.

7. REMARKS ON THE MATHEMATICAL FORMS OF POLARIMETRY CONSTRAINTS INSIDE THE EQUILIBRIUM CODES.

The previous sections contain information on the correct mathematical form to be used inside the equilibrium codes for the polarimetry constraints, for JET discharges.

In general the constraint on Faraday rotation cannot be expressed using the 'linear form ' [2.7]: the example of the calculations related to the chord#4 for shot #67777 shows that the numerical model or Type II are more adequate to describe the Faraday rotation at high density, and for shot#75238, at high current and density.

The introduction of Cotton-Mouton as constraint in the equilibrium code for an improved determination of plasma density must be treated carefully, since for Cotton-Mouton the 'linear form' can be used only at low-medium density , while at high density the effect of Faraday rotation must be included. The simplest form of a model for Cotton-Mouton, which includes the dependence upon Faraday rotation is represented by TypeII approximation.

CONCLUSIONS

This paper presents a detailed analysis of Faraday measurements at JET and comparison with available models and a rigorous approach to the interference between Faraday and Cotton-Mouton, studied in

recent papers. The Faraday rotation can be calculated from the Stokes equations and the comparison between the calculations and the measurements can lead to information related to corrections of the position of the magnetic surfaces. Moreover it turns out that the Faraday rotation cannot in general be represented by the linear expression of the TypeI approximation (expression [2.7], sec 2). The Cotton-Mouton, at high density and current, must be calculated including the dependence from the Faraday rotation angle. The present paper suggests that the test of the new mathematical forms of Faraday and Cotton-Mouton in the constraints of EFIT equilibrium code is necessary to obtain accurate equilibrium reconstructions in all JET regimes of operations.

ACKNOWLEDGEMENTS

The authors would like to thank S Segre for interesting observations and suggestions about the analysis presented in this paper; L Appel , M Brix , V Drozdov and E Solano are gratefully acknowledged for discussions about the polarimetry constraints in EFIT equilibrium code.

This work, supported by the Euratom Communities under the contract of Association between EURATOM/ENEA, was carried out within the framework the European Fusion Development Agreement. The views and opinions expressed herein do not necessarily reflect those of the European Commission.

REFERENCES.

[1]. Braithwaite G, Gottardi N, Magyar G, O'Rourke J, Ryan J and Veron D (1989) *Rev. Sci. Instrum.* **60** 2825

[2]. Orsitto F P , A Boboc, C Mazzotta, E Giovannozzi, L Zabeo and JET EFDA Contributors (2008) *Plasma Phys Contr Fusion* **50** 115009

[3]. D O'Brien and al. Nuclear Fusion 32 (1992) 1351

[4]. Guenther K et al. (2004) *Plasma Phys. Control. Fusion* **46** 1423

[5]. S E Segre and V Zanza (2006) *Plasma Phys. Control. Fusion* **48** 339

[6]. E Solano, private communication.

[7]. F Sartori , A Cenedese, F Milani Fusion Engineering and Design **66-68**(2003) 735-739

Shot #	n_{emin} (**) (10^{19} m^{-3})	n_{emax} (**) (10^{19} m^{-3})	$\int$nedl Ch3(*) (10^{19} m^{-2})	T_{emin} (keV)	T_{emax} (keV)	B_T	I_P (MA)	W_1	W_3
60980	2	3.9	4-9	1.5	3.1	1.6/2.4	2/1.6	0.016	0.25
67777	2.7	12	6-28	2.5	3.5	2.7	2.5	0.11	1.4
75238	3	10	18-20	5	6	2.75	3.4	0.08	1.4

(*) Line integrated density interval as measured by the FIR interferometer, on channel 3.

(**) Measured values of electron density by LIDAR Thomson Scattering

Table I. Plasma parameters

Diagnostic System	Measured Quantity	Symbol	Error bar
polarimeter	Faraday Rotation	ψ	0.2^o
polarimeter	Cotton-Mouton Phase shift	ϕ	2^o
LIDAR Thomson Scattering	Line integral plasma density	$\int ne\, dL$	10%
LIDAR TS	Plasma density profile	ne	5%
LIDAR TS	Plasma temperature profile	Te	10%

Table II. Error bars of measurements used in the calculations

	nmax	IP	BT
70053	1.35	3.56	3.14
70222	1.22	3	2.99
70238	0.97	2.55	2.63
70646	0.93	2.28	2.18
70691	0.9	1.85	2.26
68515	0.9	1.73	1.83
68741	0.87	1.73	1.83
70004	0.63	2.52	2.55
70206	0.41	1.22	1.9
70275	0.5	1.95	3.09
70312	0.43	1.62	2.96
70084	0.38	1.8	3.36
70558	0.28	2	2.31
70336	0.6	1.9	3
70548	0.6	2	2.7

Table III- Dataset used to study the dependence of the shift upon plasma parameters : nmax =maximun electron density in units of $10^{20}m^{-3}$;IP=plasma current in MA; BT=toroidal magnetic field in tesla.

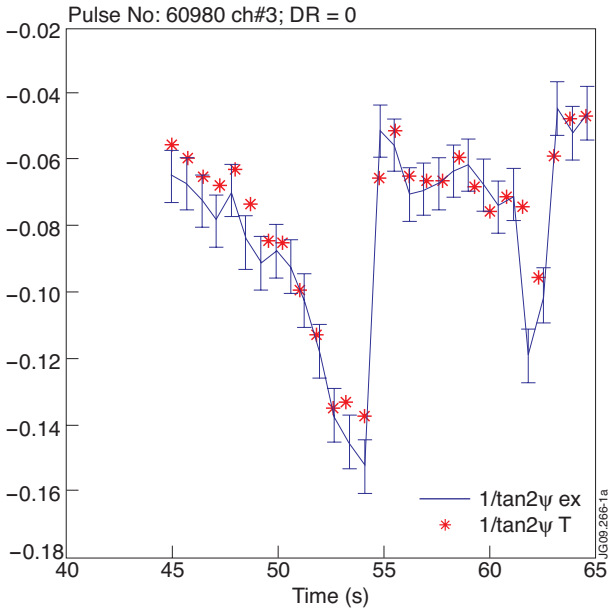

Figure 1: Faraday rotation measurement (blue continuous line, Pulse No: 60980, channel #3) is plotted together with the calculated values ('' symbol) using the numerical solution of Stokes equations. Plasma parameters are given in Table I. Agreement within the error bars.*

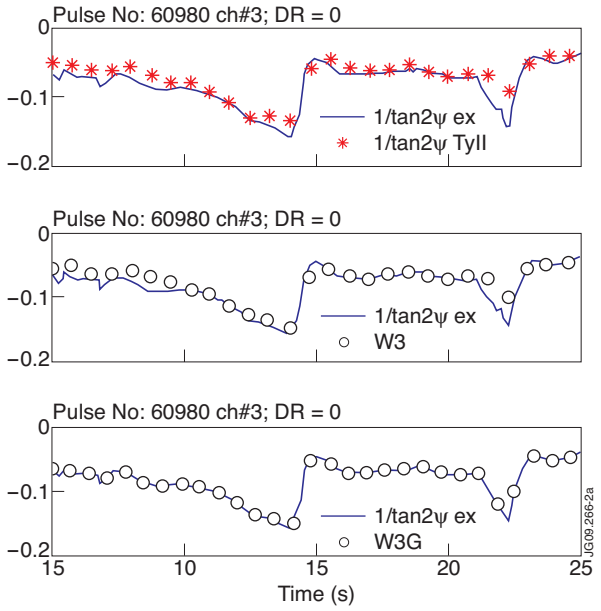

Figure 2: Faraday rotation. A complete comparison (and agreement) between the models and measurements is presented for the Pulse No: 60980, channel #3. From the top the comparison of measurements with the Type II approximation, the 'linear' W_3 approximation, and the Guenther Model A.

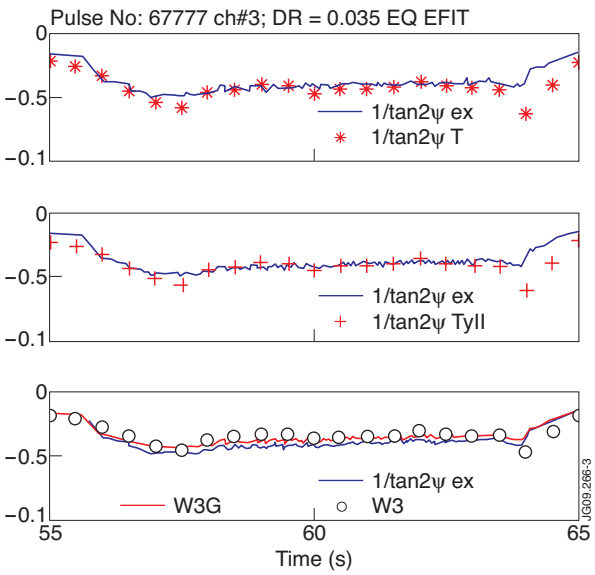

Figure 3: Faraday rotation. Similar as fig.2 , but for the high density Pulse No: 67777 and the third figure from the top reports the calculation of W3 (the linear approximation) instead of W3G (Guenther Model A): here the agreement between data and models is obtained by a rigid shift of the magnetic surfaces DR= 0.035m. The data are in agreement with all the models , in particular with the 'linear' W_3 model.

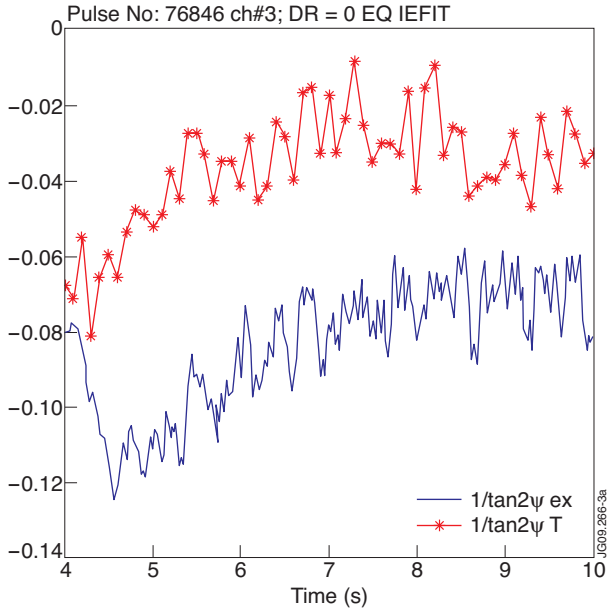

Figure 3(a): Faraday rotation.Comparison between measurements (continuous blue line) and results of numerical solution of Stokes equations (continuous red line) for Pulse No: 76846, where the shift of magnetic surfaces DR=0. The EFIT equilibrium (which includes magnetic measurements) is used without constraints(EQ IEFIT).

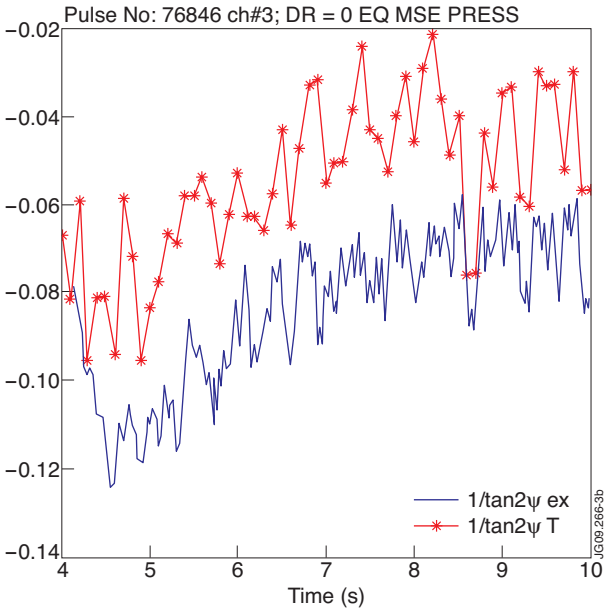

Figure 3(b): Faraday rotation.Comparison between measurements (continuous blue line) and results of numerical solution of Stokes equations (continuous red line) for Pulse No: 76846, where the shift of magnetic surfaces DR=0. The EFIT equilibrium is used with constraints including MSE(Motional Stark Effect) and pressure profile measurements(EFTM).

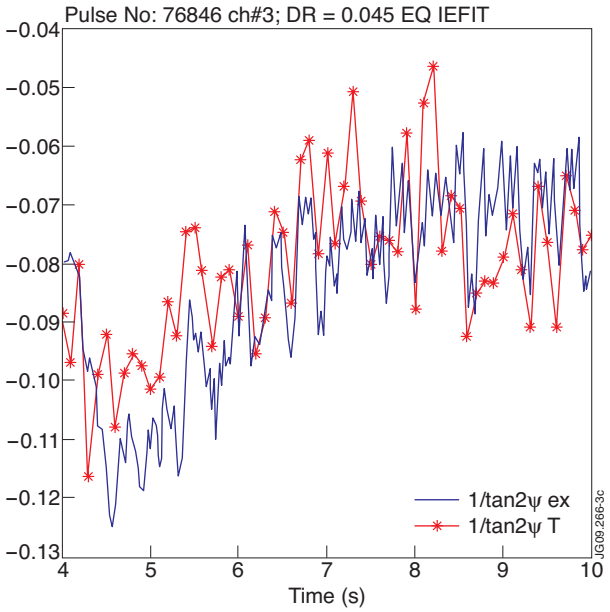

Figure 3(c): Faraday rotation.Comparison between measurements (continuous blue line) and results of numerical solution of Stokes equations (continuous red line) for Pulse No: 76846, where the shift of magnetic surfaces DR=0.045m. The EFIT equilibrium is used without constraints(EQ IEFIT).

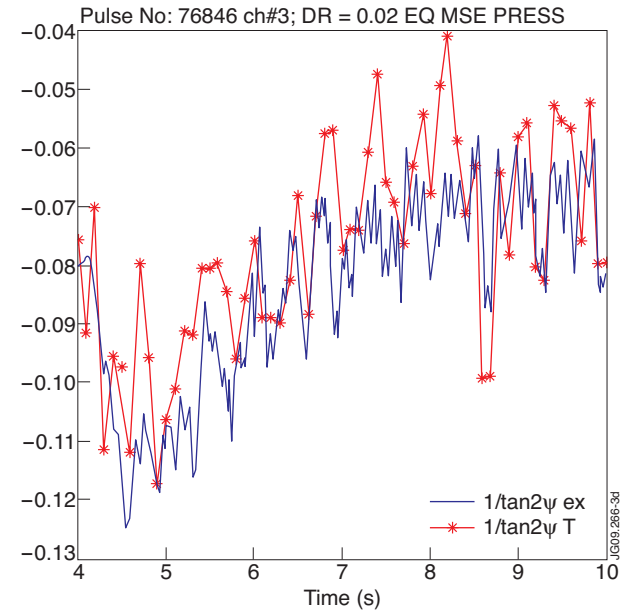

Figure 3(d): Faraday rotation.Comparison between measurements (continuous blue line) and results of numerical solution of Stokes equations (continuous red line) for Pulse No: 76846, where the shift of magnetic surfaces DR=0.02m. The EFIT equilibrium is used with constraints including MSE (Motional Stark Effect) and Thomson Scattering pressure profile measurements (EFTM).

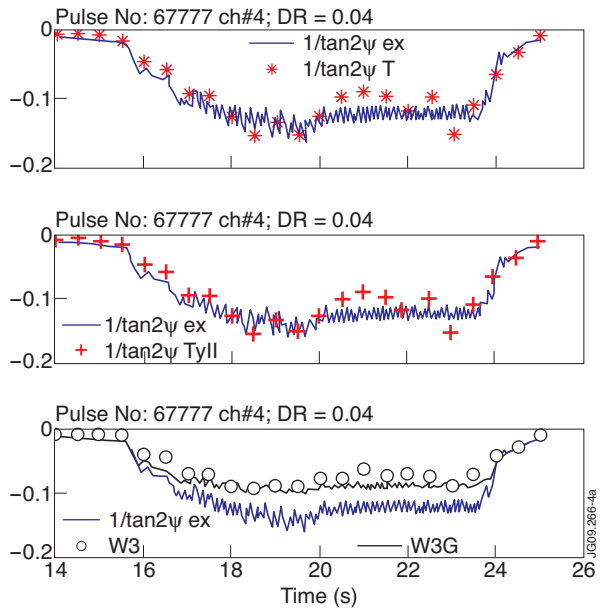

Figure 4: Faraday rotation. Comparison between models and data for Pulse No: 67777, channel #4: from the top the comparison of measurements with numerical solution , the Type II approximation, the 'linear' W_3 approximation and the Guenther Model A. Agreement between data and the Stokes numerical solutions and Type II approximation is found operating a rigid shift of 0.04m of the line of sight. The approximate values of W_3 (and Guenther Model A) slightly underestimate the measurement.

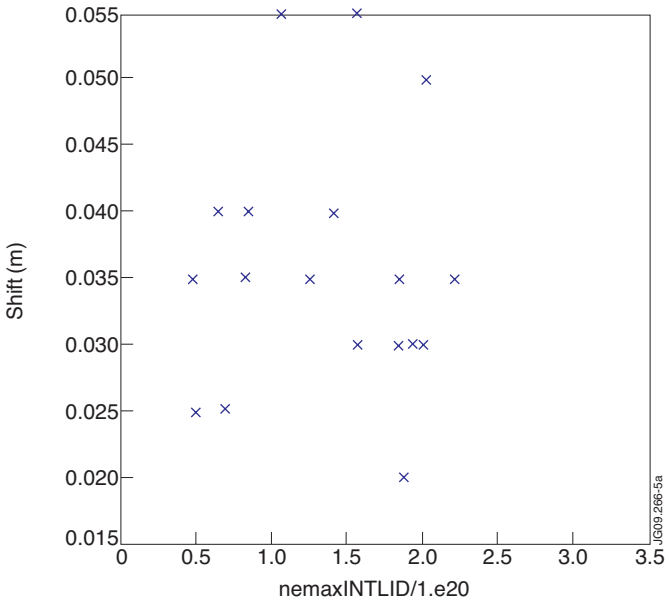

Figure 5(a): the shift (m) versus the maximum line averaged electron density measured by LIDAR Thomson Scattering in units of 1020 m-3.

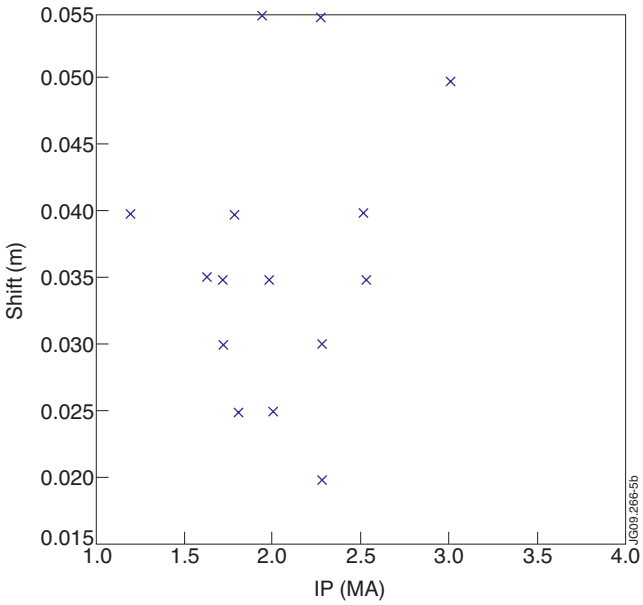

Figure 5(b): the shift(m) versus the plasma current(MA).

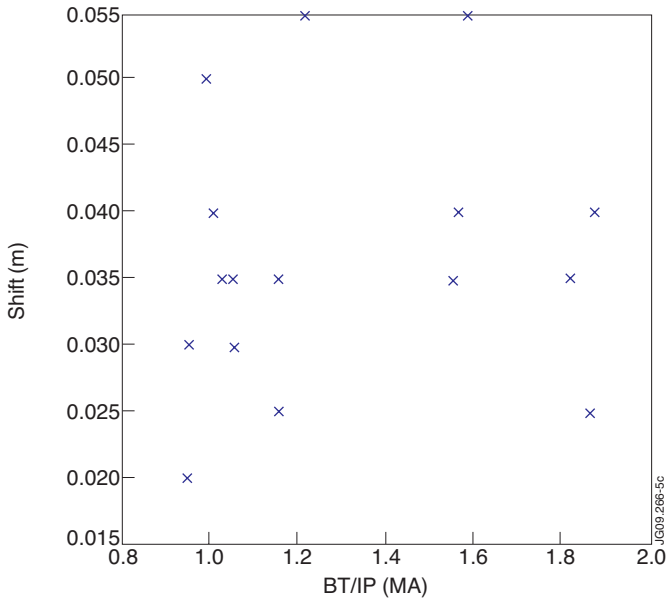

Figure 5(c): the shift versus the ratio BT/IP (toroidal magnetic field / plasma current).

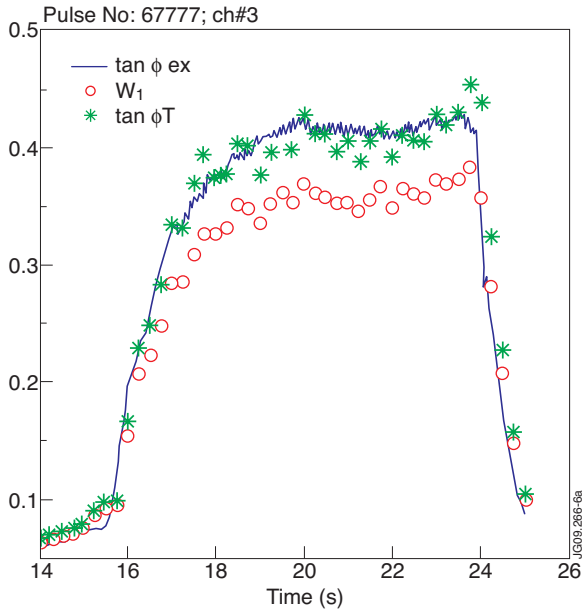

Figure 6: Cotton-Mouton.The phase shift versus time (continuous line) is compared with the numerical solution (star simbols), and the linear W_1 approximation(red circles).Pulse No: 67777, channel 3.

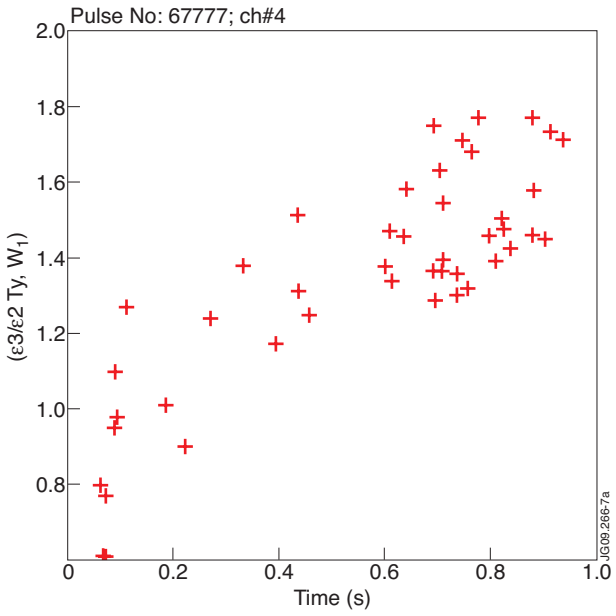

Figure 7: Cotton-Mouton. The calculated (cross symbol) (s3/s2)/W_1 versus W_3 is shown for the Pulse No: 67777, channel#3.

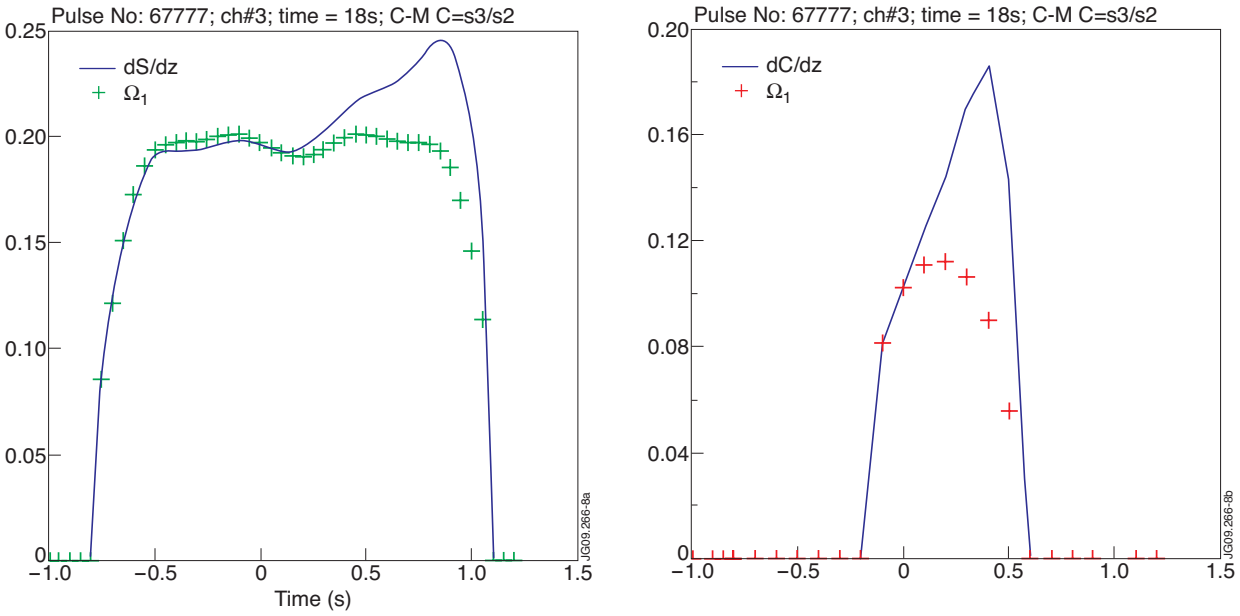

Figure 8: Cotton Mouton. The right member of equation [III.2] (blue continuous line) , and ('cross' symbols) the values of Ω_1 are shown, for the Pulse No: 67777, channel#3(fig.8a) and channel#4 (fig.8b).

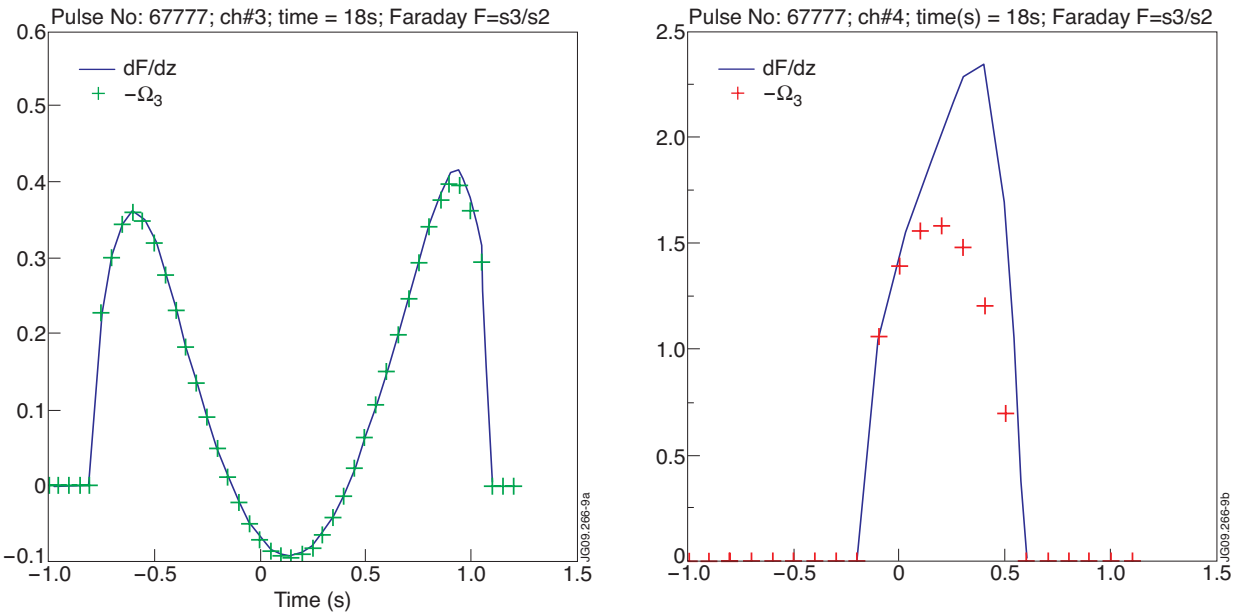

Figure 9: Faraday rotation. The right member of equation [III.1] (continuous line) , and ('cross' symbols) the values of Ω_3 are shown, for the Pulse No: 67777, channel #3 (fig.9a) and channel#4 (fig.9b).

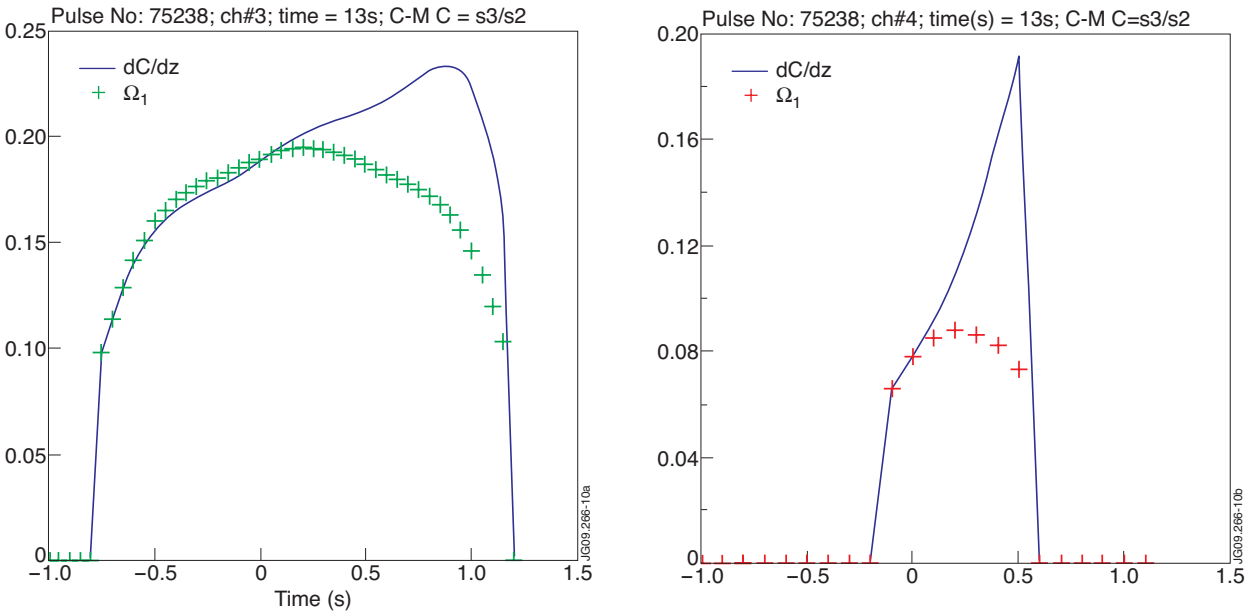

Figure 10: Cotton Mouton. The right member of equation [III.2] (blue continuous line) , and ('cross' symbols) the values of Ω_1 are shown, for the Pulse No: 75238, channel#3 (fig.10a) and channel #4 (fig.10b).

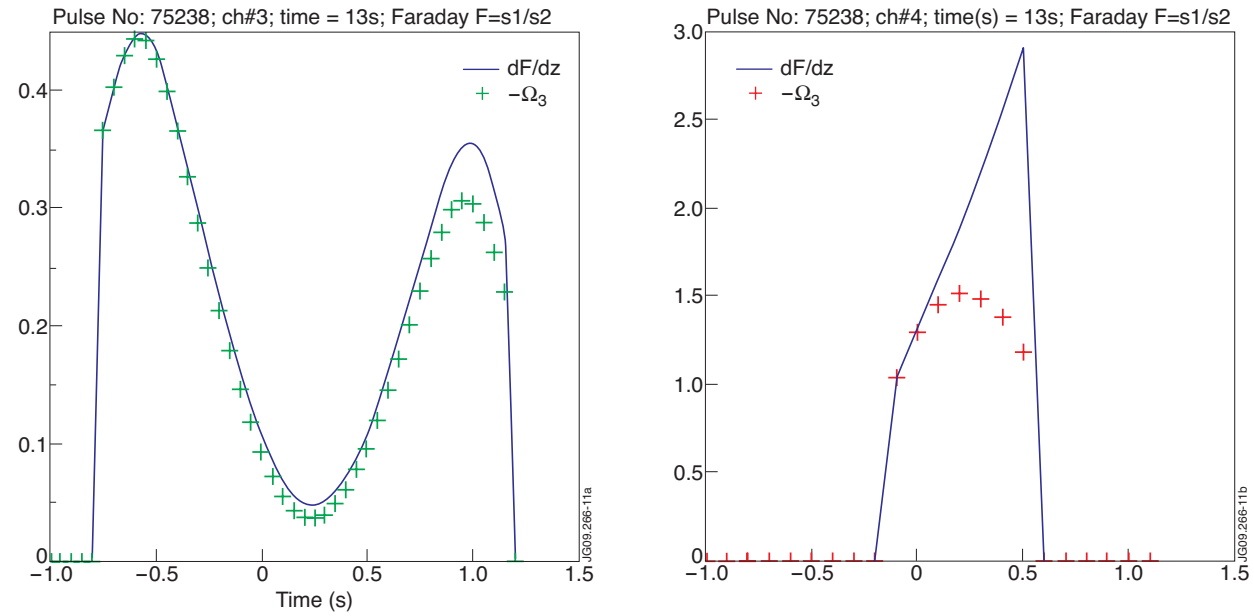

Figure 11: Faraday rotation. The right member of equation [III.1] (blue continuous line) , and ('cross' symbols) the values of Ω_3 are shown, for the Pulse No: 75238, channel #3 (fig.11a) and channel #4 (fig.11b).

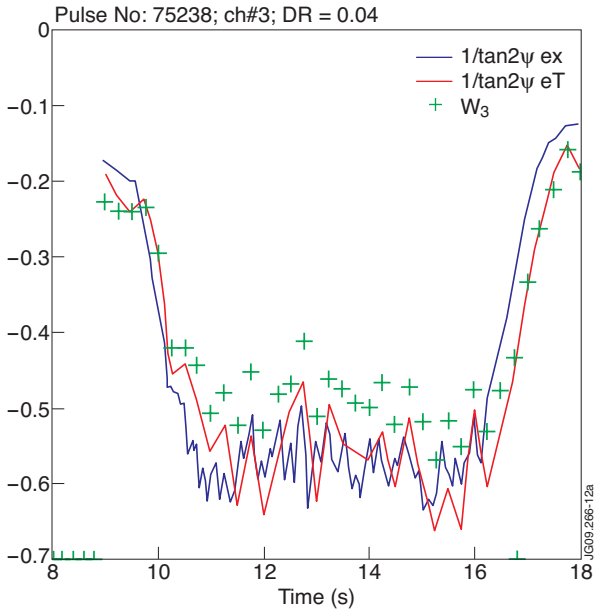

Figure 12: Faraday rotation measurement (continuous blue line, Pulse No: 75238, channel #3) is plotted together with the calculated values (continuous red line) using the solution of Stokes equations. The calculated values of W_3 are shown by green crosses.